

21. M. Yoneyama, T. Fujita, *Immunity* **29**, 178 (2008).
 22. S. Plumet et al., *PLoS One* **2**, e279 (2007).
 23. G. Luo, M. Wang, W. H. Konigsberg, X. S. Xie, *Proc. Natl. Acad. Sci. U.S.A.* **104**, 12610 (2007).
 24. C. J. Fischer, N. K. Maluf, T. M. Lohman, *J. Mol. Biol.* **344**, 1287 (2004).
 25. Materials and methods are available as supporting material on Science Online.
 26. M. U. Gack et al., *Proc. Natl. Acad. Sci. U.S.A.* **105**, 16743 (2008).
 27. S. Myong, I. Rasnik, C. Joo, T. M. Lohman, T. Ha, *Nature* **437**, 1321 (2005).
 28. S. Myong, M. M. Bruno, A. M. Pyle, T. Ha, *Science* **317**, 513 (2007).
 29. E. Jankowsky, C. H. Gross, S. Shuman, A. M. Pyle, *Science* **291**, 121 (2001).
 30. H. Durr, C. Korner, M. Muller, V. Hickmann, K. P. Hopfner, *Cell* **121**, 363 (2005).
 31. We thank C. Joo and K. Ragnathan for careful review of the manuscript. This work was supported by NIH grant R01-GM065367 and NSF Physics Frontiers Center grant 0822613 to T.H., NIH grant CA82057 to J.U.J., and a Human Frontiers of Science grant to T.H. and K.-P.H. K.-P.H. acknowledges support from the German Excellence Initiative. S.C. is supported by Deutsche Forschungsgemeinschaft (DFG) program project 455 to K.-P.H. A.K. acknowledges support from the DFG graduate school 1202. T.H. is an investigator with

the Howard Hughes Medical Institute. S.M. is a fellow at the Institute for Genomic Biology.

Supporting Online Material

www.sciencemag.org/cgi/content/full/1168352/DC1
 Materials and Methods
 Figs. S1 to S14
 References

11 November 2008; accepted 15 December 2008
 Published online 1 January 2009;
 10.1126/science.1168352
 Include this information when citing this paper.

Neuronal Activity–Induced *Gadd45b* Promotes Epigenetic DNA Demethylation and Adult Neurogenesis

Dengke K. Ma,^{1,2,*} Mi-Hyeon Jang,^{1,3*} Junjie U. Guo,^{1,2} Yasuji Kitabatake,^{1,3} Min-lin Chang,^{1,3} Nattapol Pow-anpongkul,¹ Richard A. Flavell,⁴ Binfeng Lu,⁵ Guo-li Ming,^{1,2,3} Hongjun Song^{1,2,3,†}

The mammalian brain exhibits diverse types of neural plasticity, including activity-dependent neurogenesis in the adult hippocampus. How transient activation of mature neurons leads to long-lasting modulation of adult neurogenesis is unknown. Here we identify *Gadd45b* as a neural activity–induced immediate early gene in mature hippocampal neurons. Mice with *Gadd45b* deletion exhibit specific deficits in neural activity–induced proliferation of neural progenitors and dendritic growth of newborn neurons in the adult hippocampus. Mechanistically, *Gadd45b* is required for activity-induced DNA demethylation of specific promoters and expression of corresponding genes critical for adult neurogenesis, including brain-derived neurotrophic factor and fibroblast growth factor. Thus, *Gadd45b* links neuronal circuit activity to epigenetic DNA modification and expression of secreted factors in mature neurons for extrinsic modulation of neurogenesis in the adult brain.

Adult neurogenesis represents a prominent form of structural plasticity through continuous generation of new neurons in the mature mammalian brain (1, 2). Similar to other neural activity-induced plasticity with fine structural changes within individual neurons, adult neurogenesis is modulated by a plethora of external stimuli (1, 2). For example, synchronized activation of mature dentate neurons by electroconvulsive treatment (ECT) in adult mice causes sustained up-regulation of hippocampal neurogenesis (3) without any detectable cell damage (fig. S1). How transient activation of mature neuronal circuits modulates adult neurogenesis over days and weeks is largely unknown.

Epigenetic mechanisms potentially provide a basis for such long-lasting modulation (4). We examined the expression profiles of known epigenetic regulators in response to ECT, including those involved in chromatin modification (5). One gene that we found to be strongly induced by ECT was *Gadd45b* (Fig. 1A) (6), a member of the *Gadd45* family previously implicated in DNA repair, adaptive immune response (7–10), and DNA 5-methylcytosine excision in cultured cells (11). We first characterized *Gadd45b* induction by neuronal activity in the adult hippocampus (5). Analysis of microdissected dentate gyrus tissue showed robust, transient induction of *Gadd45b* expression by a single ECT (Fig. 1A, fig. S2, and table S1). In situ analysis revealed induction largely in NeuN⁺ mature dentate granule cells (Fig. 1B and fig. S3). Spatial exploration of a novel environment, a behavioral paradigm that activates immediate early genes (IEGs) (12), also led to significant induction of *Gadd45b*, but not *Gadd45a* or *Gadd45g* (Fig. 1, C and D). Most *Gadd45b*-positive cells also expressed Arc (Fig. 1D) (88 ± 3%, n = 4), a classic activity-induced IEG. Thus, physiological stimulation is sufficient to induce *Gadd45b* expression in dentate granule cells. Experiments with pharmacological manipulations of primary hippocampal neurons further

suggested that *Gadd45b* induction by activity requires the N-methyl-D-aspartate receptor (NMDAR), Ca²⁺, and calcium/calmodulin-dependent protein kinase signaling (fig. S4 and supporting text). In vivo injection of the NMDAR antagonist +3-(2-carboxypiperazin-4-yl)-propyl-1-phosphonic acid (CPP) abolished ECT-induced *Gadd45b* and Arc expression in the adult dentate gyrus (Fig. 1E). Together, these results suggest that *Gadd45b* shares the same induction pathway as classic activity-induced IEGs (13).

We next assessed whether *Gadd45b* induction is required for neural activity–dependent adult neurogenesis. Adult *Gadd45b* knockout (KO) (10) mice appeared anatomically normal (fig. S5) and exhibited identical NMDAR-dependent induction of known IEGs at 1 hour after ECT (Fig. 1E). To examine neural progenitor proliferation, adult mice at 3 days after ECT or sham treatment were injected with bromodeoxyuridine (BrdU) and killed 2 hours later (5). Stereological counting showed similar densities of BrdU⁺ cells in the dentate gyrus between wild-type (WT) and KO mice without ECT (Fig. 2). After ECT, however, there was a 140% increase in the density of BrdU⁺ cells in WT mice and only a 40% increase in KO littermates (Fig. 2). Little caspase-3 activation was detected within the dentate gyrus under all these conditions (figs. S1 and S6), ruling out a potential contribution from cell death. To confirm this finding with a manipulation of better spatio-temporal control, we developed effective lentiviruses to reduce the expression of endogenous *Gadd45b* with short-hairpin RNA (shRNA) (fig. S7). Expression of shRNA-*Gadd45b* through stereotaxic viral injection largely abolished ECT-induced proliferation of adult neural progenitors, whereas the basal proliferation was similar to that of shRNA-control (fig. S7). We also examined exercise-induced adult neurogenesis, a physiological stimulation that induced a modest increase in *Gadd45b* expression (fig. S8A). A 7-day running program led to a marked increase of neural progenitor proliferation in adult WT mice, but was significantly less effective in their KO littermates (fig. S8B). Together, these results demonstrate a specific and essential role of *Gadd45b* in activity-induced, but not basal, proliferation of neural progenitors in the adult dentate gyrus.

We next examined the role of *Gadd45b* induction in the dendritic development of newborn

¹Institute for Cell Engineering, Johns Hopkins University School of Medicine, 733 North Broadway, Baltimore, MD 21205, USA.

²The Solomon H. Snyder Department of Neuroscience, Johns Hopkins University School of Medicine, 733 North Broadway, Baltimore, MD 21205, USA. ³Department of Neurology, Johns Hopkins University School of Medicine, 733 North Broadway, Baltimore, MD 21205, USA. ⁴Department of Immunobiology, Howard Hughes Medical Institute, Yale University School of Medicine, 300 Cedar Street, New Haven, CT 06520, USA. ⁵Department of Immunology, University of Pittsburgh, School of Medicine, Pittsburgh, PA 15261, USA.

*These authors contributed equally to this work.

†To whom correspondence should be addressed. E-mail: shongju1@jhmi.edu (H.S.); dma2@jhmi.edu (D.K.M.)

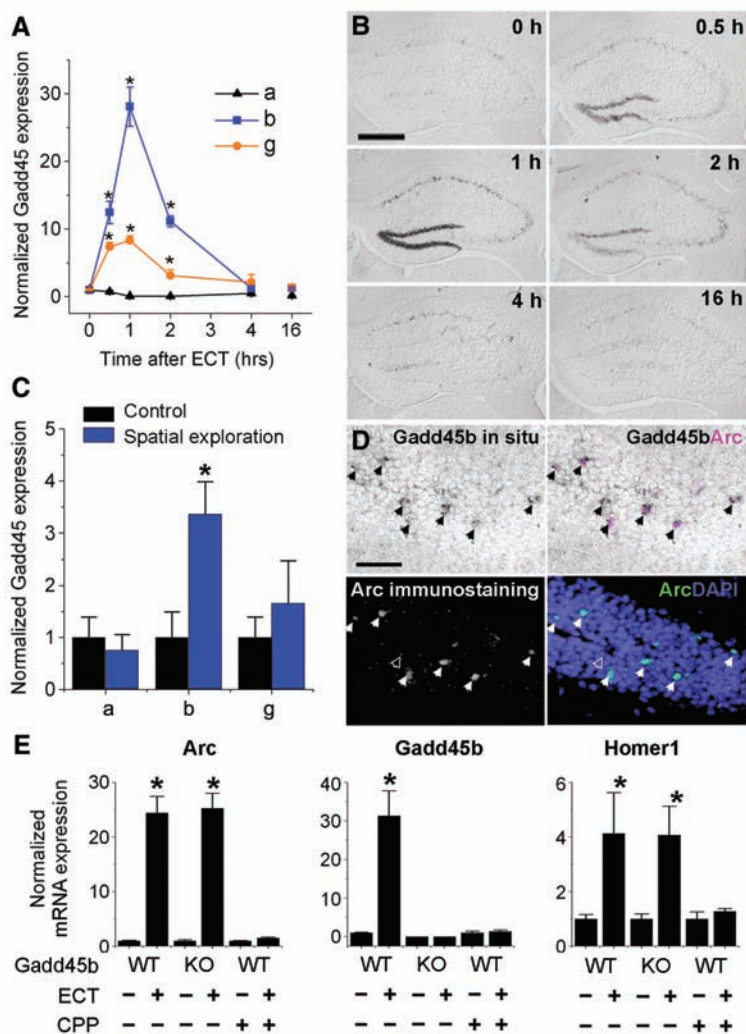


Fig. 1. Activity-induced neuronal *Gadd45b* expression. **(A)** Quantitative polymerase chain reaction (Q-PCR) analysis of ECT-induced expression of *Gadd45a*, *Gadd45b*, and *Gadd45g* in the adult dentate gyrus after a single ECT. **(B)** Sample images of *Gadd45b* in situ hybridization of the adult hippocampus after ECT. Scale bar: 0.5 mm. **(C and D)** *Gadd45* induction in the dentate gyrus after 1 hour of spatial exploration of a novel environment. **(C)** A summary from Q-PCR analysis. **(D)** Sample confocal images of *Gadd45b* in situ hybridization, and 4',6-diamidino-2-phenylindole (DAPI) and Arc immunostaining. Most of the *Gadd45b*-positive cells (open and closed arrowheads) were Arc-positive (closed arrowheads). Scale bar: 50 μ m. **(E)** NMDAR-dependent induction of *Gadd45b*, *Arc*, and *Homer1* in the adult dentate gyrus at 1 hour after ECT. The NMDAR antagonist CPP was injected intraperitoneally at 1 hour before ECT (10 mg per kg of body weight). Values represent mean \pm SEM [$n = 4$ animals; * $P < 0.01$, analysis of variance (ANOVA)].

neurons. Retroviruses expressing green fluorescent protein (GFP) were stereotactically injected into the dentate gyrus of adult WT and KO mice to label proliferating neural progenitors and their progeny (5, 14). A single ECT was given at 3 days after injection, when most GFP-labeled cells have already become postmitotic neurons (14). Quantitative analysis showed that ECT markedly increased the total dendritic length and complexity of GFP⁺ newborn neurons at 14 days after retroviral labeling (Fig. 3). This ECT-induced dendritic growth was significantly attenuated in KO mice, whereas the basal level of dendritic growth was similar (Fig. 3). Thus, *Gadd45b* is also essential for activity-induced dendritic development of newborn neurons in the adult brain.

How does transient *Gadd45b* induction regulate activity-dependent adult neurogenesis over the long-term? *Gadd45a* has been implicated in promoting global DNA demethylation in cultured cells, yet the finding remains controversial (11, 15). To examine whether *Gadd45b* induction may confer long-lasting epigenetic modulation in the expression of neurogenic niche signals, we analyzed DNA methylation status using microdissected adult dentate tissue enriched in NeuN⁺ mature neurons (5). No significant global DNA demethylation was detected after ECT in vivo (figs. S9 and S10B and supporting text). We next used methylated DNA immunoprecipitation (MeDIP) analysis in a preliminary screen for region-specific DNA demethylation, with a focus on growth factor families that have been implicated in regulating adult neurogenesis (2). Significant demethylation was found at specific regulatory regions of brain-derived neurotrophic factor (*Bdnf*) and fibroblast growth factor-1 (*Fgf-1*) (fig. S10B). Bisulfite sequencing analysis further confirmed ECT-induced demethylation within the regulatory region IX of *Bdnf* (16) and the brain-specific promoter B of *Fgf-1* (17) (Fig. 4, A and B; fig. S11 and table S2). Every CpG site within these regions exhibited a marked reduction in the frequency of methylation (Fig. 4A). Time-course analysis further revealed the temporal dynamics of DNA methylation status at these CpG sites (figs. S12 and S13). In contrast, no significant change was induced by ECT in the pluripotent cell-specific *Oct4* promoter or the kidney and liver-specific *Fgf-1G* promoter (18)

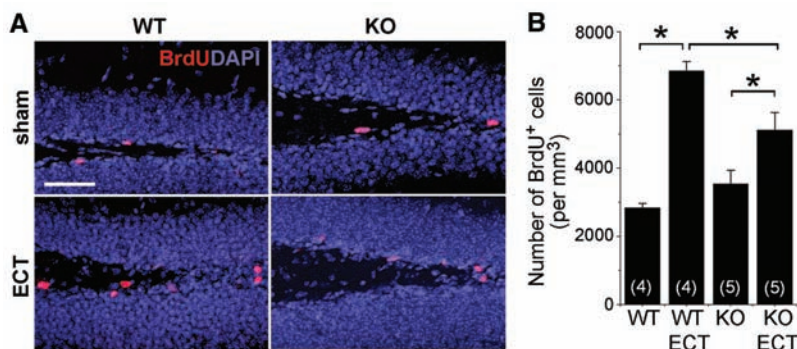


Fig. 2. Essential role of *Gadd45b* in activity-induced proliferation of adult neural progenitors. **(A)** Sample projected confocal images of BrdU immunostaining (red) and DAPI (blue). Scale bar: 50 μ m. **(B)** Summary of stereological quantification of BrdU⁺ cells in the dentate gyrus. Values represent mean \pm SEM ($n = 4$ or 5 animals as indicated; * $P < 0.01$, ANOVA).

(Fig. 4B and fig. S11B). Comparison of adult *Gadd45b* WT and KO mice without ECT showed no significant difference in the basal lev-

els of DNA methylation within *Bdnf* IX and *Fgf-1B* regulatory regions (Fig. 4B and fig. S14). In contrast, ECT-induced DNA demethylation

of these regions was almost completely abolished in KO mice (Fig. 4, A and B, and figs. S10C and S11A). In addition, overexpression of *Gadd45b* appeared to promote DNA demethylation in vivo (Fig. 4C) and to activate methylation-silenced reporters in cultured postmitotic neurons (fig. S15). Chromatin immunoprecipitation analysis further showed specific binding of *Gadd45b* to the *Fgf-1B* and *Bdnf* IX regulatory regions (fig. S16). ECT-induced gene expression from these regions and total expression of *Bdnf* and *Fgf-1* were largely absent in *Gadd45b* KO mice at 4 hours (Fig. 4D and fig. S17), consistent with a critical role of DNA methylation status in regulating gene expression. Thus, *Gadd45b* is essential for activity-dependent demethylation and late-onset expression of specific secreted factors in the adult dentate gyrus.

In summary, *Gadd45b* links neuronal circuit activity to region-specific DNA demethylation and expression of paracrine neurogenic niche factors from mature neurons in controlling key aspects of activity-dependent adult neurogenesis (fig. S18). As endogenous target of *Gadd45b*-dependent demethylation pathway, BDNF is known to promote dendritic growth of neurons in vivo, and FGF-1 exhibited as robust mitogenic activity as FGF-2 on neural progenitor proliferation in vitro (fig. S19). The presence of *Gadd45b* in chromatin associated with *Bdnf* IX and *Fgf-1B* regulatory regions in neurons (fig. S16) points to its direct role in gene regulation and potentially in a demethylation complex (fig. S18) (11, 19). The known role of the *Gadd45* family in 5-methylcytosine excision (7, 8, 11) is consistent with the emerging notion that region-specific demethylation can be mediated through DNA repair-like mechanisms, as supported by genetic and biochemical studies in both *Arabidopsis* and mammalian cells (20, 21) (supporting text).

How transient neuronal activation achieves long-lasting effects in neural plasticity and memory has been a long-standing question; enzymatic modification of cytosine in DNA was proposed as a means to provide such necessary stability with reversibility (22). Although DNA demethylation can occur passively during cell division, emerging evidence suggests the existence of active demethylation in postmitotic cells (23–25). DNA demethylation in neurons represents an extra layer of activity-dependent regulation, in addition to transcription factors and histone-modifying enzymes (13). *Gadd45b* expression is altered in some autistic patients (26) and is induced by light in the suprachiasmatic nucleus (27), by induction of long-term potentiation in vivo (28). *Gadd45b* is also associated with critical-period plasticity in the visual cortex (29). Thus, *Gadd45b* may represent a common target of physiological stimuli in different neurons in vivo, and mechanisms involving epigenetic DNA modification may be fundamental for activity-dependent neural plasticity.

Fig. 3. Essential role of *Gadd45b* in activity-induced dendritic development of newborn neurons in the adult brain. (A) Sample projected Z-series confocal images of GFP⁺ dentate granule cells at 14 days after viral labeling. Scale bar: 50 μ m. (B) Quantification of the total dendritic length of GFP⁺ dentate granule cells. Values represent mean \pm SEM ($n = 23$ to 45 neurons for each condition; * $P < 0.01$, ANOVA). (C) Analysis of dendritic complexity of the same group of cells as in (B). Values represent mean \pm SEM (* $P < 0.01$, Student's *t* test).

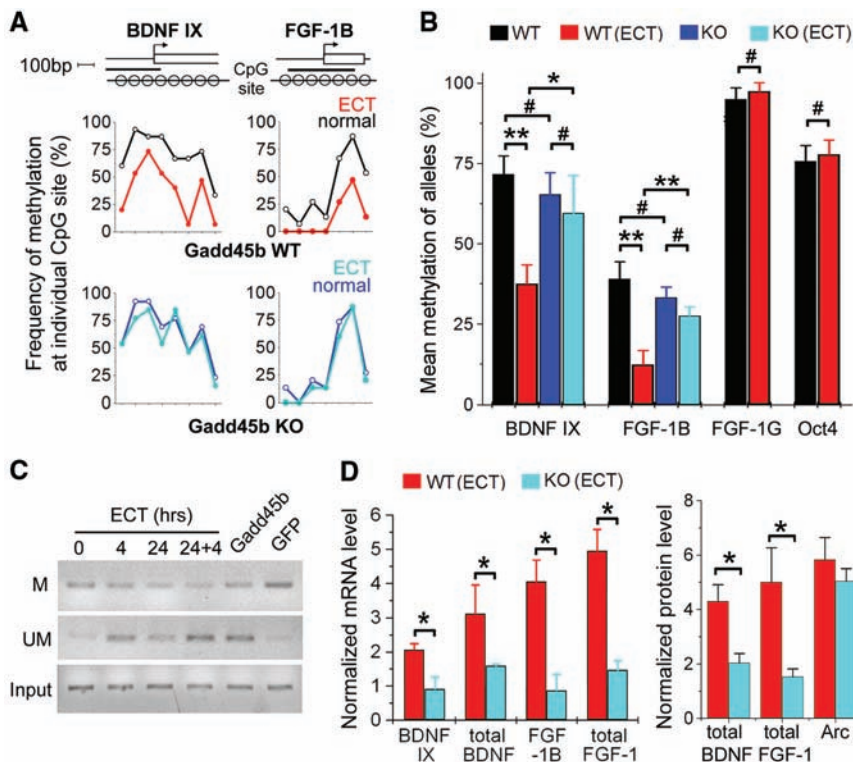
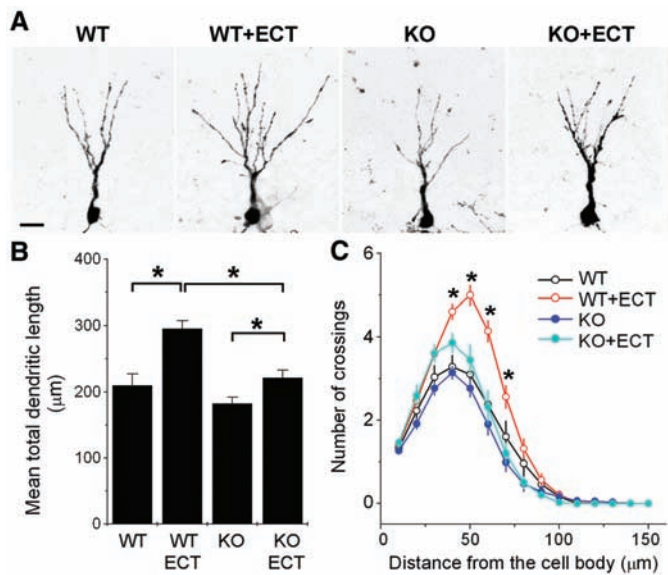


Fig. 4. Essential role of *Gadd45b* in activity-induced specific DNA demethylation and gene expression in the adult dentate gyrus. (A and B) Bisulfite sequencing analysis of adult dentate gyrus tissue before or at 4 hours after ECT. (A) A schematic diagram of the genomic region subjected to analysis and a summary of methylation frequency at individual CpG sites. (B) A summary of mean DNA methylation levels of individual alleles. Values represent mean \pm SEM ($n = 10$ to 15 reads; ** $P < 0.01$, * $P < 0.05$, # $P > 0.1$, ANOVA; exact *P* values are given in table S2). (C) Methylation-specific PCR analysis from the dentate gyrus of WT mice after one or two ECTs ("24+4": 4 hours after two ECTs at 24 hours apart) or 7 days after lentivirus-mediated expression of *Gadd45b*-GFP or GFP alone without ECT. Primers are specific for methylated (M) and unmethylated alleles (UM) of the *Fgf-1B* promoter, or for bisulfite sequencing without CpGs (Input). (D) Summary of the mRNA and protein expression in the dentate gyrus of adult *Gadd45b* WT and KO mice at 4 hours after ECT and sham controls. Values represent mean \pm SEM ($n = 4$ animals; * $P < 0.01$, ANOVA).

References and Notes

- G. Kempermann, H. van Praag, F. H. Gage, *Prog. Brain Res.* **127**, 35 (2000).
- G. L. Ming, H. Song, *Annu. Rev. Neurosci.* **28**, 223 (2005).
- T. M. Madsen et al., *Biol. Psychiatry* **47**, 1043 (2000).
- R. Jaenisch, A. Bird, *Nat. Genet.* **33** (suppl.), 245 (2003).
- Materials and methods and supporting data are available on Science Online.
- J. E. Ploski, S. S. Newton, R. S. Duman, *J. Neurochem.* **99**, 1122 (2006).
- H. J. Jung et al., *Oncogene* **26**, 7517 (2007).
- H. Tran et al., *Science* **296**, 530 (2002).
- M. C. Hollander, A. J. Fornace Jr., *Oncogene* **21**, 6228 (2002).
- B. Lu, A. F. Ferrandino, R. A. Flavell, *Nat. Immunol.* **5**, 38 (2004).
- G. Barreto et al., *Nature* **445**, 671 (2007).
- V. Ramirez-Amaya et al., *J. Neurosci.* **25**, 1761 (2005).
- S. W. Flavell, M. E. Greenberg, *Annu. Rev. Neurosci.* **31**, 563 (2008).
- S. Ge et al., *Nature* **439**, 589 (2006).
- S. G. Jin, C. Guo, G. P. Pfeifer, *PLoS Genet.* **4**, e1000013 (2008).
- T. Aid, A. Kazantseva, M. Piirsoo, K. Palm, T. Timmusk, *J. Neurosci. Res.* **85**, 525 (2007).
- K. Y. Alam et al., *J. Biol. Chem.* **271**, 30263 (1996).
- Y. Zhang, F. Madiari, K. V. Hackshaw, *Biochim. Biophys. Acta* **1521**, 45 (2001).
- N. Cervoni, M. Szyf, *J. Biol. Chem.* **276**, 40778 (2001).
- M. Gehring et al., *Cell* **124**, 495 (2006).
- R. Métévier et al., *Nature* **452**, 45 (2008).
- R. Holliday, *J. Theor. Biol.* **200**, 339 (1999).
- K. Martinowich et al., *Science* **302**, 890 (2003).
- I. C. Weaver et al., *Nat. Neurosci.* **7**, 847 (2004).
- F. D. Lubin, T. L. Roth, J. D. Sweatt, *J. Neurosci.* **28**, 10576 (2008).
- K. Garbett et al., *Neurobiol. Dis.* **30**, 303 (2008).
- V. M. Porterfield, H. Piontkivska, E. M. Mintz, *BMC Neurosci.* **8**, 98 (2007).
- D. Hevroni et al., *J. Mol. Neurosci.* **10**, 75 (1998).
- M. Majdan, C. J. Shatz, *Nat. Neurosci.* **9**, 650 (2006).
- We thank D. Ginty, S. Synder, and members of Ming and Song laboratories for help and critical comments and L. Liu and Y. Cai for technical support. This work was supported by NIH, McKnight, and NARSAD (to H.S.) and by NIH, March of Dimes, and Johns Hopkins Brain Science Institute (to G.-L.M.). R.A.F. is an investigator with the Howard Hughes Medical Institute.

Supporting Online Material

www.sciencemag.org/cgi/content/full/1166859/DC1

Materials and Methods

SOM Text

Figs. S1 to S19

Tables S1 and S2

References

6 October 2008; accepted 16 December 2008

Published online 1 January 2009;

10.1126/science.1166859

Include this information when citing this paper.

Harmonic Convergence in the Love Songs of the Dengue Vector Mosquito

Lauren J. Cator,^{1*} Ben J. Arthur,^{2*} Laura C. Harrington,¹ Ronald R. Hoy^{2†}

The familiar buzz of flying mosquitoes is an important mating signal, with the fundamental frequency of the female's flight tone signaling her presence. In the yellow fever and dengue vector *Aedes aegypti*, both sexes interact acoustically by shifting their flight tones to match, resulting in a courtship duet. Matching is made not at the fundamental frequency of 400 hertz (female) or 600 hertz (male) but at a shared harmonic of 1200 hertz, which exceeds the previously known upper limit of hearing in mosquitoes. Physiological recordings from Johnston's organ (the mosquito's "ear") reveal sensitivity up to 2000 hertz, consistent with our observed courtship behavior. These findings revise widely accepted limits of acoustic behavior in mosquitoes.

Mosquito-borne diseases such as malaria, yellow fever, and dengue continue to afflict millions, even after decades of work to control vector populations. Despite this effort, basic aspects of mosquito biology are not fully understood, including mating behavior, an important target for vector control. We describe investigations in *Aedes aegypti* that require revision of the current understanding of mosquito mating behavior. Since Johnston (*J*) first suggested in 1855 that mosquitoes could perceive sound, over 14 studies have been published on sound production and hearing in *A. aegypti* (2–17) (table S1). The buzz of a flying female mosquito acts as a mating signal, attracting males. Typically, the behaviorally salient frequency component of flight tone is the fundamental frequency of wing beat, which is between 300 to 600 Hz depending on species (8). However, mate attraction is not simply a matter of a male passively hearing and homing in on a 400-Hz tone. For example, males and females of the non-blood-feeding mosquito *Toxorhynchites brevipalpis* mod-

ulate their 300- to 500-Hz wing beat frequencies to match each other (18). Thus, acoustically mediated mate attraction involves active modulation by both sexes, creating a duet.

We show that males and females of the dengue and yellow fever vector *A. aegypti* also modulate their flight tones when brought within a few centimeters of each other. This modulation, however, does not match the fundamental wing beat frequency of around 400 Hz (female) or around 600 Hz (male) but a shared harmonic frequency of around 1200 Hz (Fig. 1). Consistent with this, a neurophysiological examination of the ears of *A. aegypti* shows response in both males and females up to 2000 Hz (Fig. 2). These results are unexpected because over 5 decades of behavioral and physiological studies had concluded that male mosquito ears (antennae and associated Johnston's organ) are tuned to 300 to 800 Hz and deaf to frequencies above 800 Hz (8, 19). The present study also directly addresses the issue of auditory competence in female mosquitoes. Acoustic duetting behavior in the nonvector mosquito *T. brevipalpis* (18) would seem to imply active audition in both sexes, and laser vibrometry studies of the Johnston's organ in that species and *A. aegypti* (16, 17) indicate that they respond mechanically to salient sounds. Moreover, female frog-biting mosquitoes are reported to be

attracted by the sounds of their singing hosts (20). The auditory physiology on *A. aegypti* provides direct evidence that females can hear and puts to rest textbook wisdom that females are deaf (8, 9).

For behavioral experiments, we tethered each mosquito to the end of an insect pin. When suspended in midair, flies initiated bouts of wing-flapping flight. We recorded flight tones with a particle velocity microphone. Acoustic interaction was demonstrated by moving a tethered flying mosquito past a stationary tethered flying partner (movie S1 with audio). Females were brought in and out of the male hearing range (2 cm) for 10-s fly-bys. Recordings revealed acoustic interaction: In 14 of 21 (67%) pairs, both sexes altered their flight tones so that the male's second harmonic [fundamental (F0) = 636.7 ± 15.1, second harmonic (F1) = 1238.3 ± 31.0 (SEM) Hz] matched the female's third harmonic [F0 = 430.6 ± 10.8, F2 = 1356.2 ± 29.2 (SEM) Hz] (Fig. 1, A to C). The period of synchronization lasted an average of 9.71 ± 1.05 (SEM) s with the synchronization frequency averaging 1354.5 ± 31.5 (SEM) Hz. *A. aegypti* do not shift their flight tones in the absence of acoustic stimulation, as tested both by deafening the mosquitoes [and stimulating with tones, Fisher's exact test, males $P = 0.02$, females $P = 0.04$ (21)] and flying intact control subjects in silence [Fisher's exact test, males $P = 0.02$, females $P = 0.04$ (21)].

The presence of the fundamental frequency tone was not necessary for harmonic matching. We stimulated tethered mosquitoes with electronically generated pure sinusoidal tones as well as with harmonic combinations of pure tones lacking the fundamental frequency (Fig. 1, D to F). The intensity of the pure tones was set at a particle velocity of 0.024 mm/s corresponding to 54 dB sound pressure level (relative to 20 μPa) when played through an ear bud speaker positioned 1.5 cm in front of the test mosquito. This intensity is well within the response range of *A. aegypti*'s Johnston's organ, as measured by Doppler vibrometry (17). Stimuli were played in 10- to 15-s bursts with 5- to 20-s recovery periods. Playback experiments with pure-tone combinations

¹Department of Entomology, Cornell University, Ithaca, NY 14853, USA. ²Department of Neurobiology and Behavior, Cornell University, Ithaca, NY 14853, USA.

*These authors contributed equally to this work.

†To whom correspondence should be addressed. E-mail: rrh3@cornell.edu